2009 American Control Conference
Hyatt Regency Riverfront, St. Louis, MO, USA
June 10-12, 2009

Why Are Some Hysteresis Loops Shaped Like a Butterfly?

Bojana Drincic and Dennis S. Bernstein

Abstract— **In this paper we investigate the origins of butterfly-shaped hysteresis maps. In particular, we show that there exist 2-to-1 maps that transform oriented simple closed curves into multi-loop closed curves with loops of opposite orientations. As an illustrative application, the hysteretic input-output map of the preloaded two-bar linkage mechanism becomes a butterfly when a 2-to-1 map is applied to it. In this case, the application of the 2-to-1 map to the hysteresis loop is equivalent to plotting an alternative output variable. We also investigate the hysteretic maps of ferroelectric materials that are transformed into a butterfly through a 2-to-1 map.**

I. Introduction

Hysteresis is a characteristic property of a nonlinear system whose periodic steady-state response retains a nontrivial input-output loop (called the hysteresis map) as the frequency of excitation approaches zero. The underlying mechanism that gives rise to hysteresis is multistability, which refers to the existence of multiple attracting equilibria. Under slow excitation, the state of the system is attracted to different equilibria depending on the direction of the input [1].

Hysteretic systems arise in a vast range of applications, such as ferromagnetics, smart materials, biological systems, and aerodynamics. In some applications, the dynamic response is independent of the frequency of excitation, and thus the dynamic response is identical to the hysteresis map. Such systems have rate-independent hysteresis. In most applications, however, the dynamic response depends on the frequency of excitation, and thus the dynamic response is distinct from the hysteresis map. Such systems have rate-dependent hysteresis. For details, see [2]. In the present paper, we focus only on the hysteresis map, that is, on the periodic steady-state response and ignore the transient response of the system.

The present paper focuses on butterfly shaped hysteresis maps, which arise in optics and smart materials [3–12]. A hysteresis map is a butterfly when it consists of two loops of opposite orientation. In many applications, the shape of the hysteresis map is reminiscent of butterfly wings, which explains the terminology.

Although butterfly hysteresis is widely observed in the literature, we are not aware of any explanations of the significance or origin of the characteristic shape of the map. In the present paper we show that any simple (that is, single-loop) hysteresis map can be transformed into a multi-loop hysteresis map with alternating loop orientation by means of a 2-to-1 mapping of the output variable. When more than two loops appear, we call the hysteresis map a multibutterfly. In particular, we provide an example in which a 2-to-1 map transforms a simple loop into a triple-loop butterfly. The extension of these ideas to n-to-1 maps is immediate.

To illustrate this phenomenon, we revisit the preloaded two-bar linkage, which is a classical example of elastic instability [13]. The hysteretic nature of this mechanism is studied in [14], where the hysteresis map is shown to be a simple closed curve in terms of the force input and linkage joint displacement. In the present paper, we consider an alternative output variable, namely, the displacement of the spring-loaded mass. In this case the resulting hysteresis map is a butterfly. This dual-loop hysteresis map with opposite orientations arises from the 2-to-1 mapping between the linkage joint displacement and the displacement of the spring-loaded mass.

The contents of the paper are as follows. In Section 2 we show that, for each oriented simple closed curve there exists a 2-to-1 map that transforms the curve into a butterfly or a multibutterfly. In Section 3 we revisit the preloaded two-bar linkage mechanism studied in [14] and demonstrate that an alternative output variable corresponds to a mapping that transforms the single-loop hysteresis map into a butterfly. In Section 4 we consider an example of hysteresis in ferroelectric materials from [3], and we find the 2-to-1 transformation map that turns the simple hysteresis loop into the butterfly.

II. Transformation from a simple curve to a multi-loop

In this section we show that for each oriented simple closed curve there exists a 2-to-1 mapping that transforms the curve into a butterfly loop. We illustrate this phenomenon with several examples.

Throughout this section, let $\mathcal{C}$ be an oriented simple closed curve and let $[F_0, F_1] \times [x_0, x_1]$ be the smallest rectangle containing $\mathcal{C}$. We assume that, for each $F \in [F_0, F_1]$, there exist at most two points $(F, x_{\min}(F))$, $(F, x_{\max}(F)) \in \mathcal{C}$, such that $x_{\min}(F) < x_{\max}(F)$. The following definitions are needed.

Definition 2.1: A continuous map $f : [x_0, x_1] \to \mathbb{R}$ is 2-to-1 if there exists $x_c \in (x_0, x_1)$ such that f is increasing on $[x_0, x_c)$ and decreasing on $(x_c, x_1]$, or vice versa.

Definition 2.2: An oriented closed curve with two loops of opposite orientation is called a *butterfly*. An oriented closed curve with three or more loops of alternating orientation is called a *multibutterfly*.

Fact 2.1: Let $f : [x_0, x_1] \to \mathbb{R}$ be a 2-to-1 map and let $[F_0, F_1] = \mathrm{cl}(\mathcal{I}_1) \cup \mathrm{cl}(\mathcal{I}_2)$, where $\mathcal{I}_1$ and $\mathcal{I}_2$

Department of Aerospace Engineering, The University of Michigan, Ann Arbor, MI 48109-2140. Tel/Fax: (734) 764-3719, (734) 763-0578 . bojanad,dsbaero@umich.edu

978-1-4244-4524-0/09/$25.00 ©2009 AACC

are disjoint open intervals. Assume that, for all $F \in \mathcal{I}_1$, $f(x_{\min}(F)) < f(x_{\max}(F))$ and, for all $F \in \mathcal{I}_2$, $f(x_{\min}(F)) > f(x_{\max}(F))$. Then $f(\mathcal{C})$ is a butterfly.

Note that $\mathrm{cl}(\mathcal{I}_1) \cap \mathrm{cl}(\mathcal{I}_2)$ is a single point.

Example 2.1: Let $\mathcal{C}$ be a circle centered at origin shown in Figure 1(a). For each value of F there are at most two corresponding values of $x(F)$. The set of points corresponding to $x_{\max}(F)$ is shown as the dashed curve, while the set of points corresponding to $x_{\min}(F)$ is shown as the solid curve. Figure 1(b) shows the 2-to-1 mapping $f(x) = 1 - |x|$ applied to $\mathcal{C}$. Note that f is continuous and increasing to the left of $x_c = 0$ and decreasing to the right of $x_c = 0$. The curve $\mathcal{C}' = f(\mathcal{C})$ is shown in Figure 1(c). However, $\mathcal{C}'$ is not a butterfly because, for all values of F in the interval $\mathcal{I}_1 = (-1, 0)$ and for all values of F in the interval $\mathcal{I}_2 = (0, 1)$, $f(x_{\max}(F)) = f(x_{\min}(F))$. In fact, $\mathcal{C}'$ is not a closed curve but rather collapses into the degenerate curve shown in Figure 1(c).

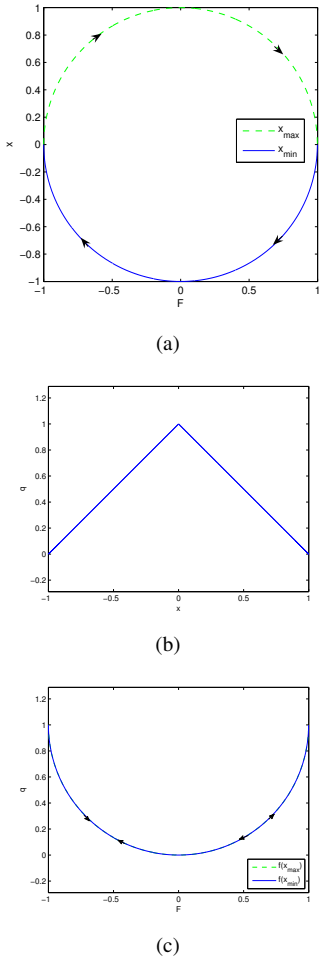

(a)

(b)

(c)

Fig. 1. Transformation that gives a degenerate curve. The original simple closed curve $\mathcal{C}$ in (a) is transformed by the mapping $f(x) = 1 - |x|$ shown in (b). The resulting curve shown in (c) is degenerate.

Example 2.2: Consider $\mathcal{C}$ shown in Figure 2(a). The set of points corresponding to $x_{\max}(F)$ is shown as the dashed line, while the set of points corresponding to $x_{\min}(F)$ is shown as the solid curve. As in Example 2.1, for each value of F there are at most two corresponding values of $x(F)$. Figure 2(b) shows the same 2-to-1 mapping f used in Example 2.1. The curve $\mathcal{C}' = f(\mathcal{C})$ is shown in Figure 2(c). However, the curve $\mathcal{C}'$ is not a butterfly because, for all F in $\mathrm{cl}(\mathcal{I}_1) \cup \mathrm{cl}(\mathcal{I}_2)$, where $\mathcal{I}_1 = (-1, 0)$ and $\mathcal{I}_2 = (0, 1)$, $f(x_{\max}(F)) > f(x_{\min}(F))$. Note that, although $\mathcal{C}'$ has two loops, both loops have the same orientation, and thus $\mathcal{C}'$ is not a butterfly.

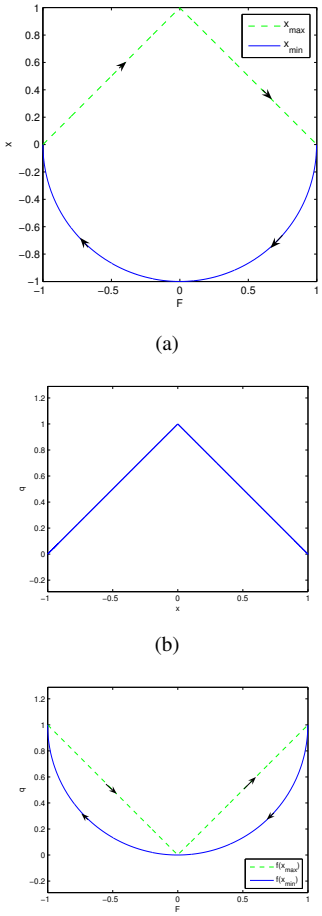

(a)

(b)

(c)

Fig. 2. Transformation that gives a two-loop curve that is not a butterfly. The original simple closed curve $\mathcal{C}$ shown in (a) is transformed by the mapping $f(x) = 1 - |x|$ shown in (b). The resulting curve shown in (c) has two loops but is not a butterfly since both curves have the same orientation.

Example 2.3: Consider $\mathcal{C}$ shown in Figure 3(a). For each value of F there are at most two corresponding values of $x(F)$. The set of points corresponding to $x_{\max}(F)$ is shown by the dashed curve, while the set of points corresponding to $x_{\min}(F)$ is shown by the solid curve. We use the same 2-to-1 mapping $f(x) = 1 - |x|$ as in the Example 2.2 (see Figure 3(b)). The curve $\mathcal{C}' = f(\mathcal{C})$ is shown in Figure 3(c). In this case, for all values of F in the interval $\mathcal{I}_1 = (-1, 0)$, $f(x_{\max}(F)) > f(x_{\min}(F))$, while, for all values of F in the interval $\mathcal{I}_2 = (0, 1)$, $f(x_{\max}) < f(x_{\min})$. Therefore, Fact 2.1 implies that $\mathcal{C}'$ is a butterfly as shown in Figure 3(c).

Fact 2.2: Let $f : [x_0, x_1] \to \mathbb{R}$ be a 2-to-1 map and

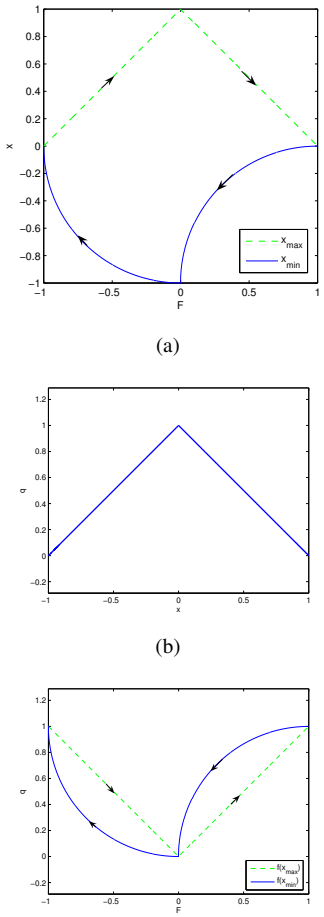

Fig. 3. Transformation of a simple curve into a butterfly. The original simple closed curve $\mathcal{C}$ shown in (a) is transformed by the mapping $f(x) = 1 - |x|$ shown in (b). The resulting curve is the butterfly loop $\mathcal{C}'$ shown in (c).

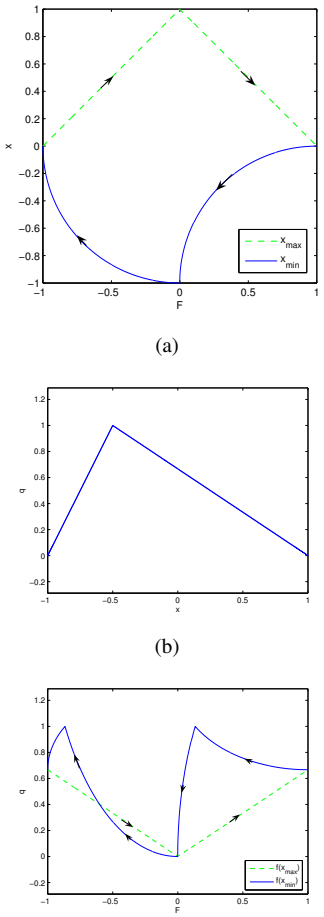

Fig. 4. Transformation of a simple closed curve into a triple loop. The counterclockwise oriented simple closed curve $\mathcal{C}$ shown in (a) is transformed by the 2-to-1 map f shown in (b). The resulting curve is the multibutterfly shown in (c).

let $[F_0, F_1] = \mathrm{cl}(\mathcal{I}_1) \cup \cdots \cup \mathrm{cl}(\mathcal{I}_n)$ where $\mathcal{I}_1, \cdots, \mathcal{I}_n$ are disjoint open intervals. Assume that, for each pair of intervals $\mathcal{I}_i, \mathcal{I}_j$ such that $\mathrm{cl}(\mathcal{I}_i) \cap \mathrm{cl}(\mathcal{I}_j) \neq \emptyset$, the following statement is true: for all $F \in \mathcal{I}_i$, $f(x_{\min}(F)) < f(x_{\max}(F))$, and, for all $F \in \mathcal{I}_j$, $f(x_{\min}(F)) > f(x_{\max}(F))$. Then $f(\mathcal{C})$ is a multibutterfly.

Example 2.4: Consider $\mathcal{C}$ as in Example 2.3 (see Figure 10(a)). The set of points corresponding to $x_{\max}(F)$ is shown by the dashed curve, and the set of points corresponding to $x_{\min}(F)$ is shown by the solid curve. Figure 10(b) shows the 2-to-1 mapping f applied to $\mathcal{C}$. The function f is continuous and increasing to the left of $x_c = -0.5$ and decreasing to the right of $x_c = -0.5$. The curve $\mathcal{C}' = f(\mathcal{C})$ is shown in Figure 4(c). For all values of F in the intervals $\mathcal{I}_1 = (-1, -0.675)$ and $\mathcal{I}_3 = (0, 1)$, $f(x_{\max}(F)) < f(x_{\min}(F))$, while, for all values of F in the interval $\mathcal{I}_2 = (-0.5, 0)$, $f(x_{\max}(F)) > f(x_{\max}(F))$. Since there are two intervals in which the order of $x_{\max}(F)$ and $x_{\min}(F)$ reverses and one in which the order remains the same, $\mathcal{C}'$ is a three-loop multibutterfly.

III. Hysteresis in a Preloaded Two-Bar Linkage Mechanism

In this section we analyze the dynamics of the two-bar linkage with joints P, Q, and R and preloaded by a stiffness k as shown in Figure 5. The purpose of this discussion is to show that the two-bar linkage is a multistable system and thus hysteretic, that is, as the frequency of excitation approaches zero the input-output loop does not vanish. We demonstrate that the shape of the hysteresis map depends on the output variable. We use the Fact 2.1 to find the 2-to-1 map that transforms the simple loop into a butterfly. Additional details of derivations are given in [14].

A constant vertical force F is applied at Q, where the two bars are joined by a frictionless pin. Let θ denote the counterclockwise angle that the left bar makes with the horizontal, and let q denote the distance between the joints P and R. When $F = 0$, the linkage has three equilibrium configurations. In Figure 6(a) and (b), the values of q and θ are q_0 and $\pm\theta_0$, respectively, and the spring k is relaxed. Note that $q_0 = 2l \cos\theta_0$. For the third equilibrium shown in

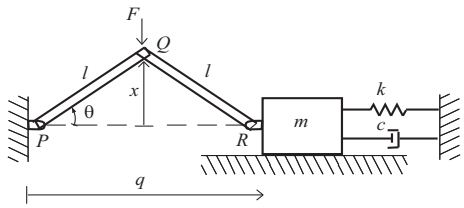

Fig. 5. The preloaded two-bar linkage with a vertical force F acting at the joint Q. The word 'preloaded' refers to the presence of the stiffness k, which is compressed when the two-bar linkage is in the horizontal equilibrium.

Figure 6(c), both bars are horizontal with $\theta = 0$.

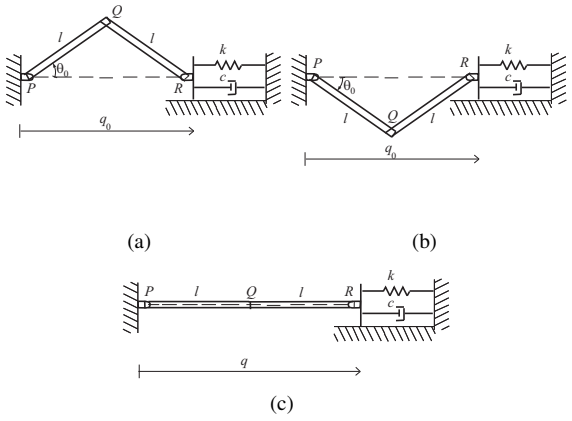

Fig. 6. Static equilibria of the preloaded two-bar linkage when the spring is relaxed and $F = 0$. In (a) the equilibrium angle θ_0 is positive, in (b) the angle is negative, and in (c) $\theta = 0$. Equilibria in (a) and (b) are stable, while the equilibrium in (c) is unstable.

The static equilibria of the system are given by

$$(\sin\theta)\left(1 - \frac{\cos\theta_0}{\cos\theta}\right) = \frac{F}{4kl}. \tag{1}$$

The equilibrium set $\mathcal{E}$ for the preloaded two-bar linkage is the set of points (F, x) that satisfy

$$x\left(1 - \frac{l\cos\theta_0}{\sqrt{l^2 - x^2}}\right) = \frac{F}{4k}. \tag{2}$$

Alternatively, set $\mathcal{E}$ can be expressed as the set of points (F, q) that satisfy

$$\pm\sqrt{(4l^2 - q^2)}\left(1 - \frac{2l\cos\theta_0}{q}\right) = \frac{F}{2k}. \tag{3}$$

Note that x is the vertical distance from the joint Q to the horizontal equilibrium, and q is the horizontal distance from joint P to joint R as shown in Figure 5. Relations (2)-(3) are obtained from (1) using

$$x = l\sin\theta, \tag{4}$$

$$q = 2l\cos\theta, \tag{5}$$

respectively.

The equilibrium sets $\mathcal{E}$ defined by (2)-(3) are shown in the Figure 7. Set $\mathcal{E}$ is useful for analyzing the hysteresis of the preloaded two-bar linkage. It is shown in [15] that a system that exhibits hysteresis has a multi-valued equilibrium map and that the hysteresis map is a subset of the equilibrium map. It can be seen from the equilibrium set $\mathcal{E}$ in Figure 7 that multiple equilibria exist for each constant $F \in (-F_{\max}, F_{\max})$.

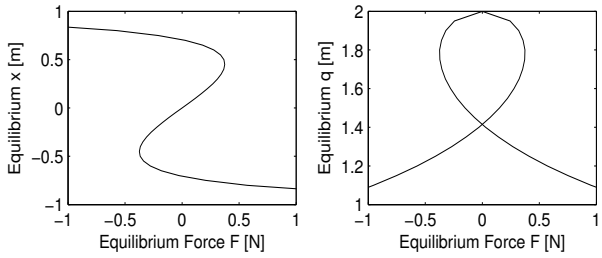

Fig. 7. Equilibrium sets $\mathcal{E}$ for the preloaded two-bar linkage. The set $\mathcal{E}$ defined by (2) is shown on the left, while the set $\mathcal{E}$ defined by (3) is shown on the right. The chosen parameter values are $\theta_0 = \pi/4$ rad, $k = 1$ N-m, and $l = 1$ m.

The equations of motion for the preloaded two-bar linkage are given by

$$\begin{aligned}\Big((2ml^2 + \frac{9}{8}m_{\rm bar}l^2)\sin^2\theta + \frac{5}{24}m_{\rm bar}l^2\Big)\ddot{\theta} \\ + (2ml^2 + \frac{9}{8}m_{\rm bar}l^2)(\sin\theta)(\cos\theta)\dot{\theta}^2 \\ + 2cl^2(\sin^2\theta)\dot{\theta} + 2kl^2(\cos\theta_0 - \cos\theta)(\sin\theta) \\ = -\frac{l\cos\theta}{2}F,\end{aligned} \tag{6}$$

where $m_{\rm bar}$ is the inertia of each bar. Using (5) the dynamics (6) can be expressed in terms of the displacement q as

$$\begin{aligned}\Big((m+\frac{9}{16}m_{\rm bar})(4l^2 - q^2) + \frac{5}{12}m_{\rm bar}l^2\Big)(4l^2 - q^2)\ddot{q} \\ + \frac{5}{12}m_{\rm bar}l^2q\dot{q}^2 + c\dot{q}(4l^2 - q^2)^2 \\ + k(q - q_0)(4l^2 - q^2)^2 = \frac{1}{2}q(4l^2 - q^2)^{\frac{3}{2}}F.\end{aligned} \tag{7}$$

We use (6) and (7) to simulate the linkage dynamics under the periodic external force $F = \sin(\omega t)$ N with parameter values $k = 1$ N/m, $m = 1$ kg, $c = 1$ N-s/m, $m_{\rm bar} = 0.5$ kg, and $l = 1$ m. As shown in Figure 8 there exists a nontrivial clockwise hysteresis map from the vertical force F to the vertical displacement x at low frequencies. The presence of a nontrivial loop at asymptotically low frequencies constitutes hysteresis. Note that the area of each hysteresis loop is equal to the energy dissipated in one cycle. Figure 9 shows the input-output map between the vertical force F and horizontal displacement q. At asymptotically low frequencies this input-output map is a symmetrical butterfly with two loops of opposite orientation. The energy dissipated in one cycle is equal to the sum of the signed areas of the two loops. Because the loops have equal area, but opposite orientation, the total energy dissipated is zero. Energy is not dissipated since the force F and the displacement q are orthogonal. A comparison of the hysteresis maps and the equilibrium sets $\mathcal{E}$ for the preloaded two-bar linkage is shown in Figure 10.

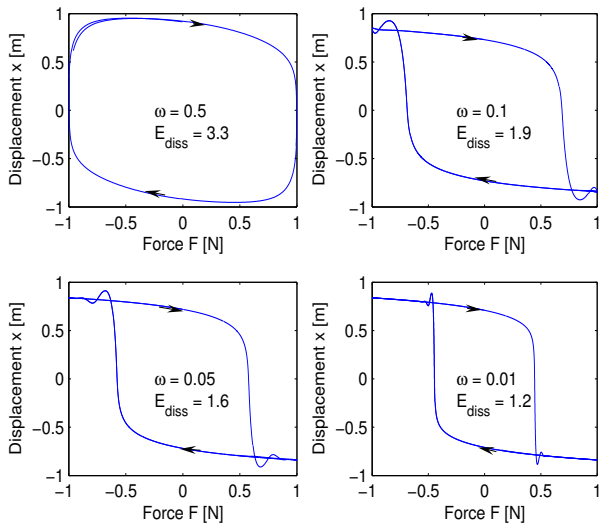

Fig. 8. Input-output maps between the vertical force F and the vertical displacement x for the two-bar linkage model (6) for several values of frequency ω in rad/s. The nonvanishing clockwise displacement-force loop at asymptotically low frequencies is the hysteresis map. $E_{\rm diss}$, which is the area of each loop, is the energy dissipated in one complete cycle. The parameters used are $k = 1$ N/m, $m = 1$ kg, $c = 1$ N-s/m, $m_{\rm bar} = 0.5$ kg, $l = 1$ m, and $F(t) = \sin(\omega t)$ N.

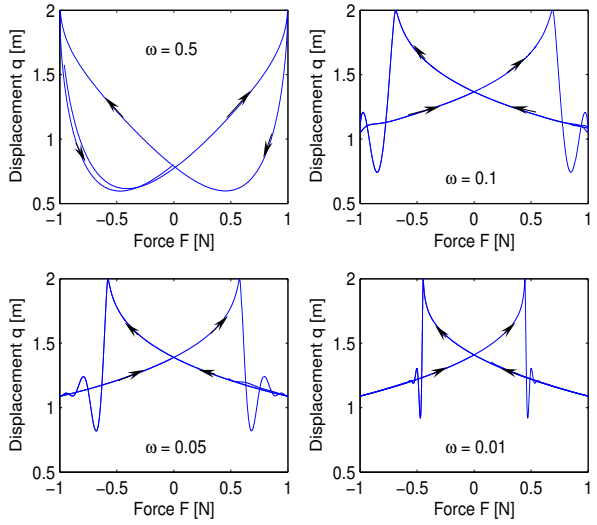

Fig. 9. Input-output maps between the vertical force F and the horizontal displacement q for the two-bar linkage model (7) for several values of frequency ω in rad/s. The parameters used are $k = 1$ N/m, $m = 1$ kg, $c = 1$ N-s/m, $m_{\rm bar} = 0.5$ kg, $l = 1$ m, and $F(t) = \sin(\omega t)$ N.

Thus the hysteresis map is a simple closed curve when the output variable is the vertical displacement x and a butterfly when the output variable is the horizontal displacement q. According to the Fact 2.1 we find the 2-to-1 map

$$f = \sqrt{4(l^2 - x^2)} \tag{8}$$

which transforms the simple loop to a butterfly and is shown in Figure 11.

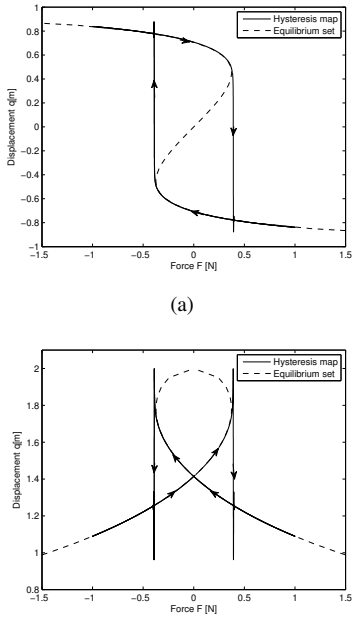

Fig. 10. Comparison of the equilibrium sets $\mathcal{E}$ and the hysteresis maps for the preloaded two-bar linkage. The output variable is x in (a) and q in (b). The hysteresis map is a subset of $\mathcal{E}$ except for the vertical segments at the bifurcation points. The parameters used are as in Figure 8 with $F(t) = \sin(0.001t)$ N.

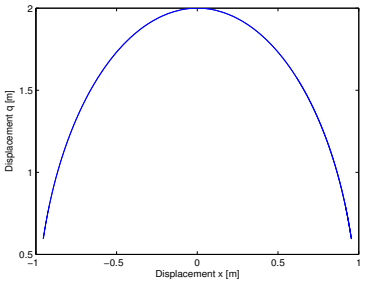

Fig. 11. The mapping function $f(x) = \sqrt{4(l^2 - x^2)}$ that transforms the simple hysteresis loop of the buckling mechanism into a butterfly.

IV. Hysteresis in Ferroelectric Materials

In this section we show that Fact 2.1 can be applied to a simple curve/butterfly pair to obtain the 2-to-1 map which relates the simple curve to the butterfly. We consider an example of hysteresis in ferroelectric materials from [3]. The actual data presented in [3] are not available, so the hysteresis loops were "extracted" from the plots given in the paper.

Ferroelectric materials are ceramics that exhibit piezoelectric behavior and can switch polarization. In an electric field ferroelectric materials change length, while under mechanical loading, ferroelectric materials change polarization. The hysteresis loop shown in Figure 12(a) represents the input-output map between the polarization P of the ferroelectric material and the applied electric field E. The butterfly shown in Figure 12(b) represents the input-output map between the length L of the specimen and the electric field E. The plots

in Figure 12 are approximations to data presented in [3].

Note that in Figure 12(a) points $P_{\max}(E)$ are shown as a dashed curve, while points $P_{\min}(E)$ appear as a solid curve. It can be concluded from Figure 12(b) that, for all E in $\mathcal{I}_1 = (E_0, E_c)$, $f(P_{\min}(E)) > f(P_{\max}(E))$, while for all E in $\mathcal{I}_1 = (E_c, E_1)$, $f(x_{\min}(F)) < f(x_{\max}(F))$, where E_0 is the minimum value of E for which the curve is defined, E_1 is the maximum value of E for which the curve is defined, and $E_c = \frac{1}{2}(E_0 + E_1)$. Thus, from Fact 2.1 it follows that there exists a 2-to-1 map f that transforms the simple hysteresis loop into a butterfly shown in Figure 12(b).

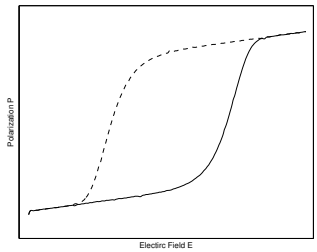

(a)

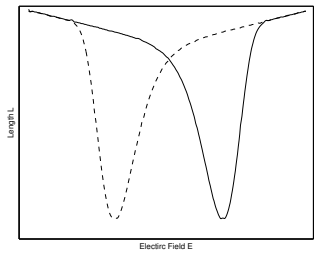

(b)

Fig. 12. Approximate hysteresis and butterfly loops for the ferroelectric specimen based on [3]. The simple hysteresis curve is the input-output map between the electric field E and polarization P shown in (a). The butterfly is the input-output map between the electric field E and the length of the specimen L shown in (b).

The 2-to-1 map f that transforms the simple loop in Figure 12(a) into the butterfly in Figure 12(b) is shown in Figure 13. The map can be computed by graphing the polarization $P(E)$ versus the length of the specimen $L(E)$. The dashed curve represents the transformation between $P_{\max}(E)$ and L, while the solid curve represents the transformation between $P_{\min}(E)$ and L. The appearance of non identical function in Figure 13 corresponding to increasing and decreasing E suggests the presence of residual dynamics due to non-quasi-static operation or numerical error.

V. Conclusion

We studied the relationship between the simple (single-loop) hysteresis maps and the butterfly hysteresis maps. We found that the simple loop and butterfly are related by a 2-to-1 map. We illustrated this point by finding the 2-to-1 map for the preloaded two-bar linkage and for ferroelectric materials.

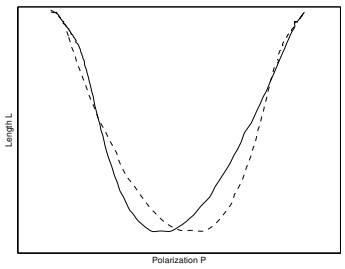

Fig. 13. The mapping f that transforms the simple hysteresis loop of ferroelectric material into a butterfly. The dashed curve represents the transformation between $P_{\max}(E)$ and L, while the solid curve represents the transformation between $P_{\min}(E)$ and L. The mismatch in the curves is due to residual dynamics or numerical error.

References

[1] D. S. Bernstein, "Ivory ghost," *IEEE Control Systems Magazine*, pp. 16–17, October 2007.

[2] J. Oh and D. S. Bernstein, "Semilinear Duhem model for rate-independent and rate-dependent hysteresis," *IEEE Trans. Autom. Contr.*, vol. 50, pp. 631–645, 2005.

[3] H. Sahota, "Simulation of butterfly loops in ferroelectric materials," *Continuum Mechanics and Thermodynamics*, vol. 16, pp. 163–175, February 2004.

[4] F. Davi, "On domain switching in deformable ferroelectrics, seen as continua with microstructure," *Zeitschrift fr Angewandte Mathematik und Physik*, vol. 52, no. 6, pp. 966–989, November 2001.

[5] C. F. Marki, D. R. Jorgesen, H. Zhang, P. Wen, and S. C. Esener, "Observation of counterclockwise, clockwise and butterfly bistability in 1550 nm VCSOAs," *Optics Express*, vol. 15, no. 8, pp. 4953–4959, April 2007.

[6] S. Ducharme, A. V. Bune, L. M. Blinov, V. M. Fridkin, S. P. Palto, A. V. Sorokin, and S. G. Yudin, "Critical point in ferroelectric Langmuir-Blodgett polymer films," *Physical Review B*, vol. 57, no. 1, pp. 25–28, January 1998.

[7] I. Chiorescu, W. Wernsdorfer, A. Muller, H. Bogge, and B. Barbara, "Butterfly hysteresis loop and dissipative spin reversal in the $S = \frac{1}{2}$, V_{15} molecular complex," *Physical Review Letters*, vol. 84, no. 15, pp. 3454–3457, April 2000.

[8] J. Li and G. J. Weng, "A micromechanics-based hysteresis model for ferroelectric ceramics," *Journal of Intelligent Material Systems and Structures*, vol. 12, pp. 79–91, February 2001.

[9] N. Ebine and K. Ara, "Magnetic measurement to evaluate material properties of ferromagnetic structural steels with planar coils," *IEEE Transaction on Magnetics*, vol. 35, no. 5, pp. 3928–3930, September 1999.

[10] P. Pakdeevanich and M. J. Adams, "Measurements and modeling of reflective bistability in 1.55-μm laser diode amplifiers," *IEEE Journal of Quantum Electronics*, vol. 35, no. 12, pp. 1894–1903, December 1999.

[11] O. Pietzsch, A. Kubetzka, M. Bode, and R. Wiesendanger, "Observation of magnetic hysteresis at the nanometer scale by spin-polarized scanning tunneling spectroscopy," *Science*, vol. 292, pp. 2053–2056, June 2001.

[12] M. Kamlah and C. Tsakmakis, "Phenomenological modeling of the non-linear electro-mechanical coupling in ferroelectrics," *International Journal of Solids and Structures*, vol. 36, no. 12, pp. 669–695, 1999.

[13] G. J. Simitses, *An Introduction to the Elastic Stability of Structures*. Englewood Cliffs, NJ: Prentice Hall, 1967.

[14] A. K. Padthe, N. A. Chaturvedi, D. S. Bernstein, S. P. Bhat, and A. M. Waas, "Feedback stabilization of snap-through buckling in a preloaded two-bar linkage with hysteresis," *Int. J. Non-Linear Mech.*, vol. 43, pp. 277–291, 2008.

[15] J. Oh and D. S. Bernstein, "Step-convergence analysis of nonlinear feedback hysteresis models," in *Proc. Amer. Contr. Conf.*, Portland, OR, June 2005, pp. 697–702.